World Academy of Science, Engineering and Technology
International Journal of Mechanical and Mechatronics Engineering
Vol:12, No:2, 2018

Prediction for the Pressure Drop of Gas-Liquid Cylindrical Cyclone in Sub-Sea Production System

Xu Rumin, Chen Jianyi, Yue Ti, Wang Yaan

***Abstract*—**With the rapid development of subsea oil and gas exploitation, the demand for the related underwater process equipment is increasing fast. In order to reduce the energy consuming, people tend to separate the gas and oil phase directly on the seabed. Accordingly, an advanced separator is needed. In this paper, the pressure drop of a new type of separator named Gas Liquid Cylindrical Cyclone (GLCC) which is used in the subsea system is investigated by both experiments and numerical simulation. In the experiments, the single phase flow and gas-liquid two phase flow in GLCC were tested. For the simulation, the performance of GLCC under both laboratory and industrial conditions was calculated. The Eulerian model was implemented to describe the mixture flow field in the GLCC under experimental conditions and industrial oil-natural gas conditions. Furthermore, a relationship among Euler number (Eu), Reynolds number (Re), and Froude number (Fr) is generated according to similarity analysis and simulation data, which can present the GLCC separation performance of pressure drop. These results can give reference to the design and application of GLCC in deep sea.

***Keywords*—**Dimensionless analysis, gas-liquid cylindrical cyclone, numerical simulation; pressure drop.

I. Introduction

As tremendous oil and gas recourses have been explored in ocean, the related marine oil exploitation has got rapid development during the previous years. In order to reduce the energy consuming, people tend to set up the production system on the ocean floor, in which an important process is the separation of the phases. As the operation conditions are restricted in the subsea area, the more compact, lightweight and robust separator is needed instead of the traditional separator. Thanks to the engineers in TULSA, a new separator named GLCC is designed and put into practice [1], [2]. GLCC is a device that uses centrifugal force and gravity to separate gas and liquid. As shown in Fig. 1, a typical GLCC consists of an inclined inlet pipe located at medium position of cylinder pipe and two outlets located at the top and the bottom of the cylinder pipe. A specific nozzle is made by cutting off the round pipe using inclined plane and make its cross section like a crescent, thus named as crescent nozzle. This crescent nozzle creates acceleration and swirl on the flow thus forming centrifugal forces which result in a vortex in the GLCC cylinder pipe. As the liquids phase may rush downwards when they enter the main pipe through the nozzle, the gases trapped in the liquids might be brought out through the bottom outlet. This phenomenon is defined as the gas carry-under GCU. In the upper part, the gas flows to the center and exits from the top, while liquid droplets are centrifuged to the cylinder pipe walls and move up toward the gas leg. This phenomenon is named as the liquid carry-over (LCO).

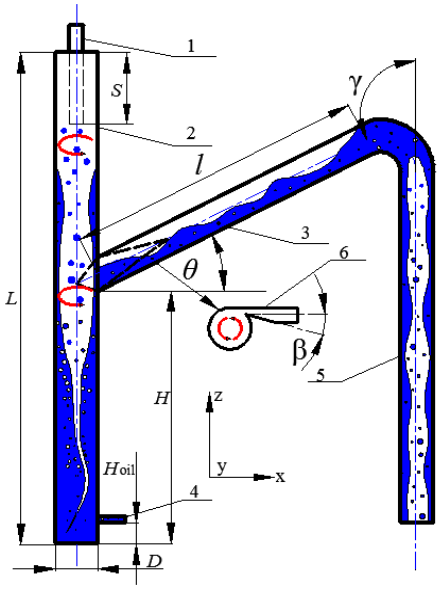

Fig. 1 The schematic of GLCC: 1. Gas outlet 2. Cylinder pipe 3. inclined downward pipe 4. liquid outlet 5. vertical inlet pipe 6. crescent nozzle

A review of the literature reveals that the complex phenomenon taking place in GLCC are still not fully understood. Especially experimental and theoretical studies on the detailed pressure drop characteristics in the GLCC are scarce. Despite the lack of pressure drop information, some studies have begun to deal with the subject and several successful studies of GLCC separators performed by the University of Tulsa. They developed mechanistic model to predict the operational envelope for LCO, GCU and separation efficiency based on experimental and theoretical studies and CFD simulation. Many researchers focus on the inclined pipe, Hreiz and Chirinos [3] observed the distribution of flow patterns in inclined inlet section by experiment, and Kouba et al. [4] presented experiments result for the effect of inlet

Xu Rumin, was with The Petroleum Institute, Abu Dhabi, 2533 UAE. Now with China university of petroleum (Beijing), MSc candidate, Beijing, 102249, People Republic of China (e-mail: xurm_cup@163.com).

Chen Jianyi is a professor at Institute of Chemical Engineering, China university of petroleum (Beijing), Beijing, 102249, People Republic of China (corresponding author, phone: 0086-10-89731519; fax: 0086-10-89731519; e-mail: jychen@cup.edu.cn).

Yue ti, PhD candidate and Wang yaan, PhD candidate. China University of Petroleum (Beijing), Beijing, 102249, People Republic of China (e-mail: 374873493@qq.com, yawang0215_cup@163.com).

inclination angle and inlet geometry on LCO. Farchi [5] measured the flow field inside the GLCC by Pitot tube. Experiments show that the swirling flow field has the characteristics of forced vortex in the small size separator. There are many researches about GLCC geometry structure; Movafaghian [6] compared the effects of double inlet structure with single inlet structure on GLCC equilibrium liquid level, null liquid holdup capacity, meteorological entrainment and operating range. It was found that dual inlet structure makes the cylinder velocity field showing a better symmetry. Erdal and Shirazi [7] used a Laser Doppler Velocimetry (LDV) to address the effect of different inlet geometries on the flow behavior of velocity components and the sum of the axial and tangential velocity fluctuations inside the GLCC.

In 1997, Erdal and Shirazi [8] simulated and compared the distribution of axial and tangential velocities in GLCC under three kinds of inlet geometry by the CFX method. Hreiz et al. [9] investigated single-phase swirl flows in a GLCC geometry numerically. They presented the comparison between different turbulence models and different near-wall treatments. Meléndez Ramírez et al. [10] considered the gas-liquid two-phase as an interpenetrating continuum using the Eulerian-Eulerian numerical simulation method. The results (interface vortex shape and liquid angular velocity) show a reasonable match with experimental data.

Although extensive research in two-phase flow pressure drop has been conducted, most of this research has concentrated on horizontal, vertical and even inclined flow. Several good correlations exist for predicting pressure drop in this horizontal, vertical and inclined flow, but these correlations cannot be successfully applied to GLCC which has a combination of these three kinds of flow. The pressure drop assigned to the GLCC by the process system is limited within off-shore installations, so we need to fully understand the effect of fluids and operating conditions to the pressure drop. In this way, adjusted operating conditions in the previous design can match the pressure afterwards. Due to the limitation of experimental conditions, it is not only expensive but also long term to study all the parameters which include physical properties of fluids, operating conditions, and geometry. Therefore, investigation using CFD method is the possible alternative.

The aim of the paper is to investigate the pressure drop of GLCC under various conditions. As the GLCC always operate with high pressure gas, it is difficult do experiments in the same environments. Therefore, numerical works are also conducted. In this paper, single phase flow and gas-liquid two phase flow in GLCC were investigated experimentally and numerically for several experimental conditions. Grid independence was obtained from the results and comparison between experimental and simulation data was conducted. The simulation on the flow of the natural gas and oil in GLCC in the real industry conditions was also conducted. The results are helpful for the design of the GLCC under different conditions.

II. Experimentation

A. Experimental Set-Up

The configuration for the experiments on GLCC is shown in Fig. 2. Pure water was initially used in the experiments. The liquids flow in a closed loop. The centrifugal pump linked with the storage tank can provide a maximum flow rate of 7 m^3/h. The storage tank allows removing the entrapped bubbles and thus protected the pump. The liquid flow rate is measured by a calibrated turbine flowmeter (Fig. 2). The gas phase is air. An air compressor provides air at a maximum relative pressure of 50 kPa and a maximum flow rate of 320 m^3/h which means that the GLCC operates almost at atmospheric pressure. The air flow rate is measured by a calibrated vortex flow meter. Several valves are used to regulate the flow rates of both phases. Incoming liquid and gas lines are connected to the GLCC inlet channel though a T-junction. The gas-liquid two-phase mixture enters the GLCC body through a crescent nozzle.

The main dimensions of the CLCC used in the experiments are shown in Fig. 3. The internal diameter of the main body of the GLCC is 74 mm, and its height is 2420 mm. The angle of inclined inlet pipe is 27° downward, its length is 1565 mm and its internal diameter is 54 mm. The structure of the crescent nozzle is shown in Fig. 4. The cross-section of the nozzle that connects to the inclined pipe remains spherical with an inner diameter of 54 mm, while it shrinks gradually and ends up with a crescent shape at junction with the main body. For a better visualization, the GLCC body is transparent and was manufactured in Plexiglas. Several holes were drilled at different parts of the GLCC to install pressure sensors (Fig. 3). In this experiment, the flow rate of gas and liquid and pressure drop are measured by Digital Data Acquisition System.

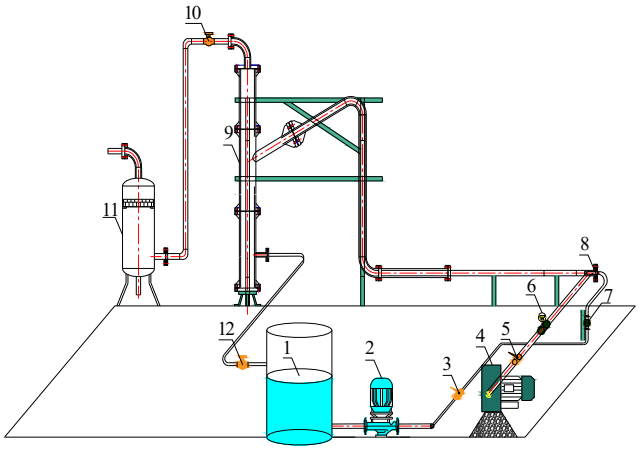

Fig. 2 Experimental set-up of GLCC. 1-Water tank, 2-Pump, 3-Liquid inlet valve, 4-Centrifugal fan, 5-Gas inlet valve, 6-Vortex flow meter, 7-Turbine flow meter, 8-Gas-liquid mixer, 9-GLCC, 10-Gas outlet valve, 11-Liquid trapper, 12-Liquid outlet valve

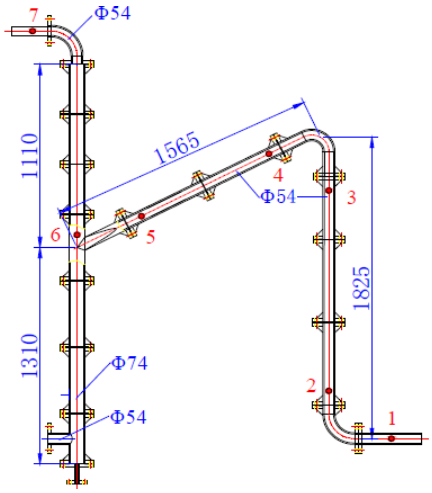

Fig. 3 The main dimensions of GLCC (mm)

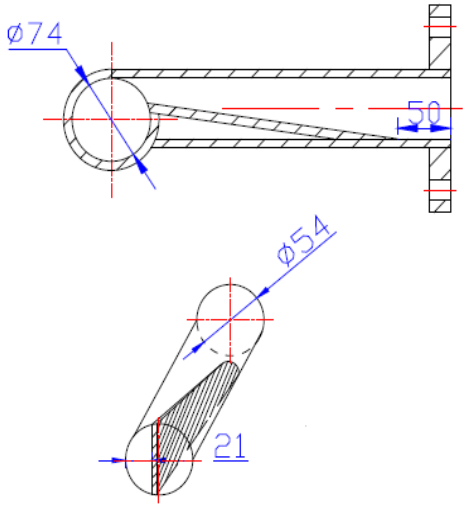

Fig. 4 Main dimension of Crescent nozzle (mm)

B. Dimensionless Analysis of GLCC

In this section, we would like to investigate the factors that influence the pressure consuming of the GLCC. As dimensionless analysis was widely used in the related area, it is convenient to quantify a performance using dimensionless groups, which reduces the number of independent variables and enhances the generality of results. The pressure drop of GLCC needs to be correlated with hydrodynamics. There are no guidelines available for the definition of dimensionless numbers for two phase GLCC as they are adapted from single phase system based either on physical properties of continuous phase or average properties of two fluids. The commonly used definitions for gas-liquid flow are shown in Table I.

The most important dimensionless number for characterization of all type of flows is Reynolds Number (Re) which relates inertial force to viscous force. Thus, it was used to predict flow patterns of the two phases in GLCC for various conditions. As previously reported, the balance between the forces generated by the radial pressure gradient and gravity are mostly responsible for the elevation of the liquid film above the nozzle centerline. Thus, the gravity was considered to have effects on the transformation of the flow pattern in GLCC. As Froude number reflects the relative importance of the gravity in the process, it was introduced as well for the prediction of the performance of the GLCC.

TABLE I
DETAILS OF DIMENSIONLESS NUMBER TO CHARACTERIZE TWO-PHASE FLOW

Dimensionless number	function	note
Re_g	$Re_g = \frac{\rho_g v_g D}{\mu_g}$	vg: velocity inlet, m/s; D: inlet pipe diameter, m; ρ_g: gas density, kg/m^3; μ_g: gas viscosity, Pa·s.
Fr_g	$Fr = \frac{gl}{v_g^2}$	g: gravitational acceleration, m/s^2; l: cylinder diameter, m; vg: velocity inlet, m/s.
Eu_g	$Eu = \frac{\Delta P}{\rho_g v_g^2}$	P: static pressure, Pa; ρ_g: gas density, kg/m^3; vg: velocity inlet, m/s.
α	$\alpha = \frac{Q_{Vl}}{Q_{Vg} + Q_{Vl}}$	α: volume fraction; Q_{Vl}: liquid volume, m^3/s; Q_{Vg}: gas volume, m^3/s.

The pressure drop is mainly focus on gas phase since the liquid fraction is too low to contribute much for it. Eu_g is a dimensionless number connected with gas phase pressure. The pressure drop model has been established as follows:

$$Eu_g = f(Re_g, \alpha, Fr_g)$$

III. NUMERICAL SIMULATION

A. Selection of the Numerical Schemes

The suitability of different numerical schemes has been intensively studied by Kaya and Karagoz [11] for highly complex swirling flows for separators with tangential inlet. It was reported that the presence of high-pressure gradients and double-vortex flow structure requires an efficient algorithm for the accuracy of the pressure computation. The PRESTO (Pressure Staggered Option) pressure interpolation scheme is successful in this respect. Among many schemes, the SIMPLEC (Semi–Implicit Method Pressure-Linked Equations Consistent) algorithm for pressure velocity coupling and the (QUICK) Quadratic Upstream Interpolation for Convective Kinetics scheme for momentum equations give a better prediction for the final results that match the experimental data. The optimum choice seems to be the second order for turbulent kinetic energy and the first order for Reynolds stresses. The numerical settings that applied for the current simulations are given in Table II.

TABLE II
THE USED NUMERICAL SETTINGS FOR THE CURRENT SIMULATIONS

Parameter	Numerical Setting
Pressure discretization	PRESTO
Pressure velocity coupling	SIMPLEC
Reynolds stress	Second order upwind
Momentum discretization	QUICK
Turbulent kinetic energy	Second order upwind
Turbulent dissipation rate	Second order upwind

B. Geometry and Boundary Conditions

The boundary conditions should be defined prior to the proper calculation. It is obvious that the initial setting of the boundary will have an important influence on the result since

it affects the iterations a lot. The boundary conditions for the flow of the pure gas and the gas-liquid two-phase are set as follows:

1) Pure Gas Simulation

In this section, the boundary conditions for the single phase flow are presented. Both the flow of the air in the experimental condition and the natural gas under industrial conditions were simulated. For the flow of air, the simulation was conducted in normal temperature and pressure (1.013×10^5 Pa). The air has the density and viscosity 1.25 kg/m^3 and the viscosity is 1.8×10^{-5} Pa.s. To ensure accordance with the actual flow pattern of industrial field, the gas flow rate is determined as 0 to 320 m^3/h. For the flow of natural gas, the boundary conditions are the same to the industrial fields, the maximum processing capacity of GLCC is 1.42×10^6 m^3/d. The upstream pressure is 10 MPa, and the inlet temperature is 46 ˚C. The natural gas has a density of 107 kg/m^3 and a viscosity of 1.5×10^{-5} Pa.s. The pure gas simulation boundary conditions are summarized in Table III:

TABLE III
BOUNDARY CONDITIONS OF SINGLE PHASE

item	air	Natural gas
Fluids	$\rho = 1.225\text{kg/m}^3$; $\mu = 1.8\times10^{-5}\text{Pa}\cdot\text{s}$	$\rho = 107\text{kg/m}^3$; $\mu = 1.5\times10^{-5}\text{Pa}\cdot\text{s}$
Velocity inlet	$V_{in} = 8.78$ to 23.22m/s I=0.16 Re$^{(-0.125)}$ DH=0.054m	$V_{in} = 2$ to 6m/s I=0.16 Re$^{(-0.125)}$ DH=0.054m
Outlet Wall	Outflow Standard wall function	Outflow Standard wall function

2) Gas-Liquid Two Phase Simulation

For the case of the gas-liquid two phase flow, two cases were simulated: one is the flow of air and water in the experimental condition, the other is the flow of the natural gas and the oil in the conditions of industrial fields. The boundary conditions for these two cases are shown in Table IV.

TABLE IV
BOUNDARY CONDITIONS OF GAS-LIQUID TWO-PHASE

Item	Air and water	Natural gas and oil
Fluids	$\rho_G = \frac{1.225\text{kg}^3}{\text{m}}$; $\mu_G = 1.8\times10^{-5}\text{Pa}\cdot\text{s}$ $\rho_L = \frac{1000\text{kg}^3}{\text{m}}$; $\mu_L = 0.000897\text{Pa}\cdot\text{s}$	$\rho_G = \frac{107\text{kg}^3}{\text{m}}$; $\mu_G = 1.5\times10^{-5}\text{Pa}\cdot\text{s}$ $\rho_L = \frac{753\text{kg}^3}{\text{m}}$; $\mu_L = 0.0007\text{Pa}\cdot\text{s}$
Velocity inlet	$V_{in} = 7$ to $\frac{22\text{m}}{\text{s}}$ $\alpha = 1$ to 6% I=0.16 Re$^{(-0.125)}$ DH=0.054m	$V_{in} = 2$ to $\frac{6\text{m}}{\text{s}}$ $\alpha = 1$ to 6% I=0.16 Re$^{(-0.125)}$ DH=0.054m
Outlet Wall	Outflow Standard wall function	Outflow Standard wall function

C. CFD Grid

As shown in Fig. 5, a 3D geometric model using software of SolidWorks is established, and the grid is generated using the commercial pre-processing software ICEM. The GLCC is divided firstly by the method of block division, and then, the structural hexahedron element is generated by O-block method. The detail of meshing at GLCC nozzle is shown in Figs. 6 and 7:

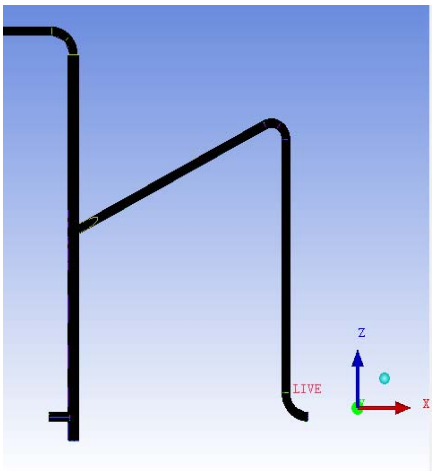

Fig. 5 The geometric model of GLCC

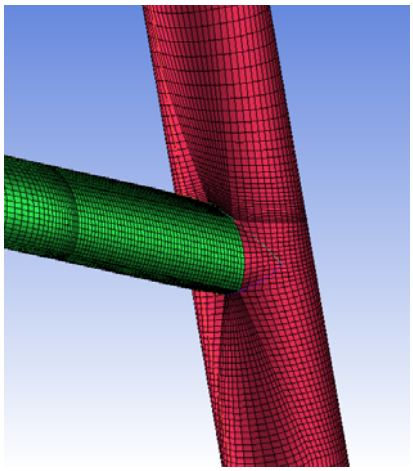

Fig. 6 Detailed grid of crescent nozzle (on back side)

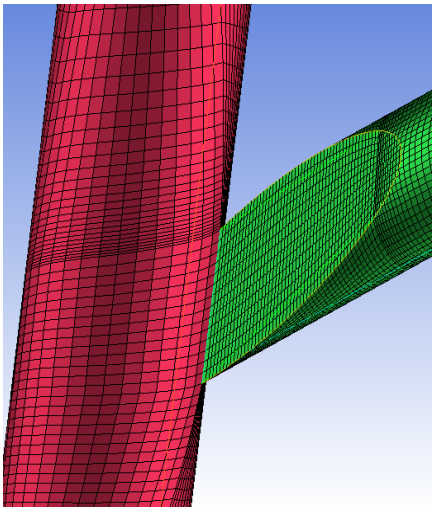

Fig. 7 Detailed grid of crescent nozzle (front side)

D. Grid Independence

Grid independence is associated with the accuracy of the

final numerical results. Typically, a sequence of the coarse, medium and fine meshes will be built for the purpose of showing that the solution changes little between medium and fine mesh. In this paper, three levels of grid for each cyclone have been tested, which are 43488, 445172, and 599694 cells, to be sure that the obtained results are grid independent. The computational results of the three grid types are presented in Fig. 8. It can be seen from the figure that the total pressure drop with a grid number of 43488 is significantly different with grid number of 445172 and 599694. Therefore, for excluding any uncertainty, computations have been performed using 445172 cells grid, where the total number of grids was not that critical with respect to the computation overhead.

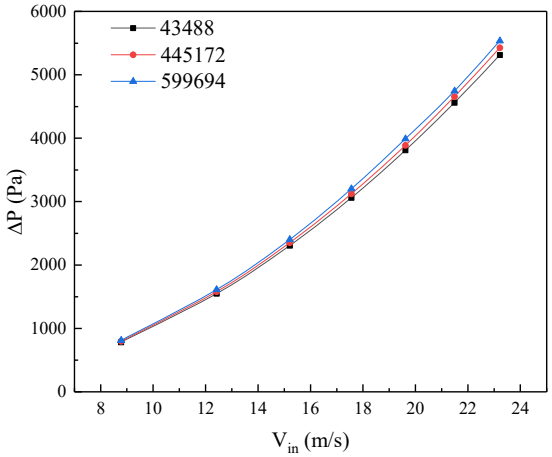

Fig. 8 Comparison of ΔP in different grid number

E. Validation of the Numerical Model

In order to validate the obtained results, it is necessary to compare the prediction with experimental data. The present simulation is compared with the measured pressure drop. The pressure drop of the GLCC is defined as the pressure difference between the inlet and the average pressure across the vortex finder exit. In the experiment, pressure drop of the GLCC was calculated by the difference between the pressures at the inlet and gas outlet. In this paper, the simulation of both the single phase and the gas-liquid two phase were validated by the comparison of pressure drop for CFD prediction and experimental data.

1) Comparison of Single Phase Simulation

Fig. 9 shows a comparison of the pressure drops obtained from the experiment and the CFD prediction for different inlet air velocities. As mentioned before, Eu can be used to indicate the pressure drop of the GLCC, thus the evolutions of Eu against Re obtained by both experiments and the simulations were plotted in Fig. 9. As seen, the maximum difference between the results is less than 5%, therefore, the above comparison results show that the numerical model employed in the study can be used to analyze the performance of the GLCC for single phase simulation.

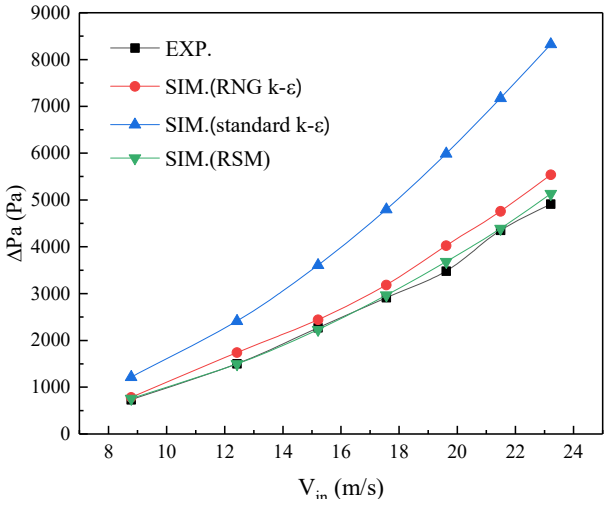

Fig. 9 Comparison of the ΔP between experiments and CFD simulations for different inlet air velocity

2) Comparison of Gas-Liquid Two Phase Simulation

Fig. 10 shows a comparison of the pressure drops obtained from the experimental data and CFD simulation. A small deviation from the experimental values was observed in the calculated pressure drop. And the Eulerian model matches the experimental pressure drop with underestimation of the pressure drop especially in lower air velocities. This may be caused by the limitation of Eulerian model. In Eulerian model, the droplet is regarded as a spherical particle while we ignore the fragmentation and coalescence of droplet in the actual motion. In addition, it appears from the figure that the trend of CFD simulation and experiment is consistent. Therefore, considering the complexity of the turbulent swirling gas-liquid two-phase flow in the GLCC, the agreement between the simulations and measurements is considered to be quite acceptable.

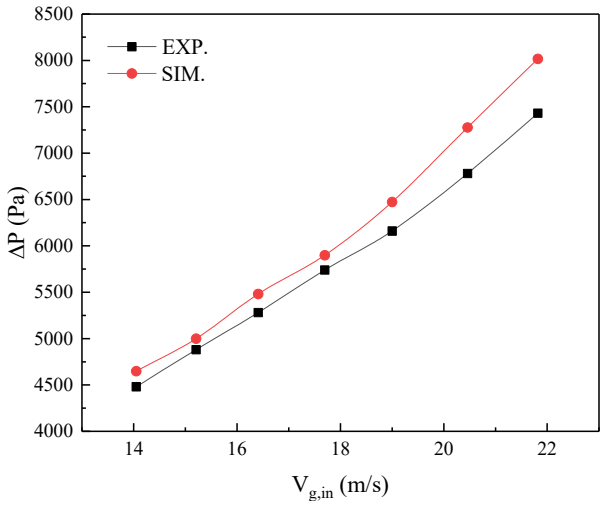

Fig. 10 Comparison of ΔP between experiments and CFD simulations for different inlet air velocity (Q_L=0.3 m^3/h)

IV. Results

A. Prediction for the Pressure Drop for Single Phase

As discussed before, Eu was picked to indicate the pressure drop in GLCC. Since the pressure drop is mainly induced by the gas phase, which occupies larger volume in the GLCC, the Eu number based on the gas phase was calculated. The evolution of the Eu number for the single phase, including the single air and the single natural gas, against the Reynolds number is exhibited in Fig. 11. One can find that the Eu decreases rapidly with the increase of the Re for the single air due to the small value of the Re. While, Re becomes much larger for the nature gas in the real industrial condition. However, the difference of Eu number between air and natural gas is slightly small which is only 3.7%. That is because in self-stimulated domain (High Re, Re>1×10^5), the Eu number will not change with Re. Accordingly, the Eu decreases smoothly.

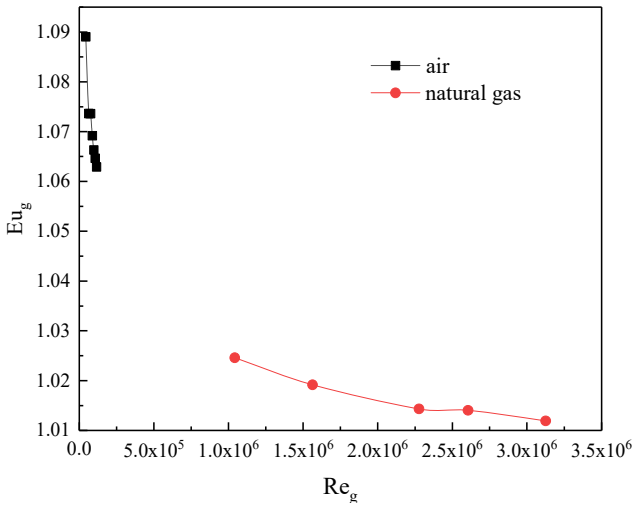

Fig. 11 The relationship between gas Eu number and Reynolds number for air and natural gas

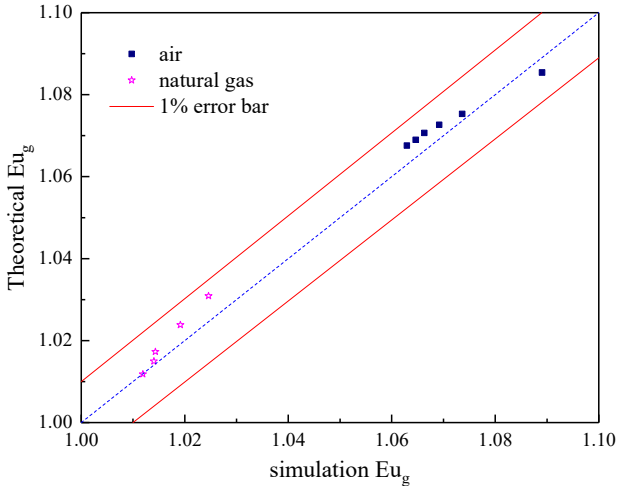

Fig. 12 Comparison of the model value and simulation data

Froude number Fr_g was introduced to indicate the effect of the gravity on the pressure drop of the GLCC. For the flow of the single gas phase, the prediction model for the pressure drop can be assumed as following:

$$Eu_g = k_1 Re_g^{k_2} Fr_g^{k_3}$$

Here, k_1, k_2 and k_3 are constant coefficients that indicate the relative importance of each number. According to the relevant data, we obtained that k_1=1.300, k_2=-0.017, k_3=-0.026. The model value and experimental data that are shown in Fig. 11 have a high correlation coefficient of above 0.9899 (Fig. 12), which can be used to predict the pressure drop of the GLCC for the real industrial application.

B. Pressure Drop of Gas-Liquid Two-Phase Flow

1) Air-Water Two-Phase Flow in GLCC

Fig. 13 shows the trend of the Euler number of the gas phase Eu_g with the Reynolds number Re_g when the volume fraction of the liquid phase is 1%, 2%,3%,4%, 5%,6%. As can be seen from the figure, the Euler number of the gas phase Eu_g gradually decreases with the increase of the Reynolds number of the gas phase. And all the cases tend to follow the same slope at last. Fig. 14 shows the relationship between gas Euler number Eu_g, and liquid volume fraction when the Reynolds number of gas is 35040, 50058, 75086, and 110126. It can be seen from the figure that the variation of Euler number Eu_g with liquid phase volume fraction approaches the linear relationship. And the slopes corresponding to each line are approximately equal.

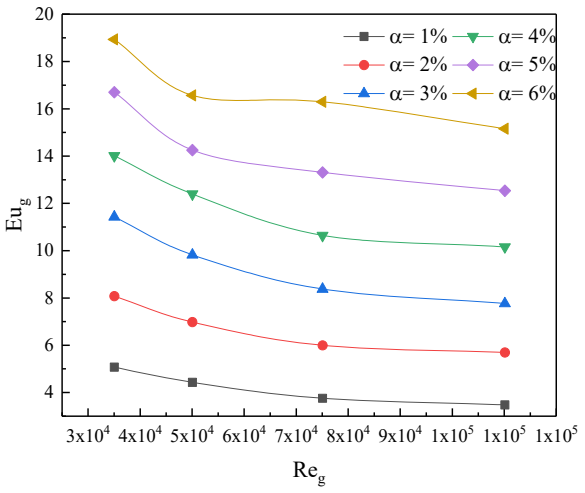

Fig. 13 Relationship between Eu_g and Re_g of GLCC

Under air-water two-phase flow, the pressure drop prediction model can be assumed as following:

$$Eu_g = k_1 \alpha^{k2} \mathrm{Re}_g^{\ k3} Fr_g^{k4}$$

k_1, k_2, k_3 and k_4 are constant coefficients. For the case of the single phase flow, k_2=0; for the case of gas-liquid two phase, $k_2 \neq 0$, in addition, there is a relationship between Eu_g and a

$^{6.34}$*Re_g*$Fr_g^{0.5}$ as shown in Fig. 15. Therefore, the mechanistic model is just like as following:

$$Eu_g = 26.017\alpha^{0.805}\left(Re_g\sqrt{Fr_g}\right)^{-0.1270} 3.5\times10^4 < Re_g < 1.1\times10^5$$

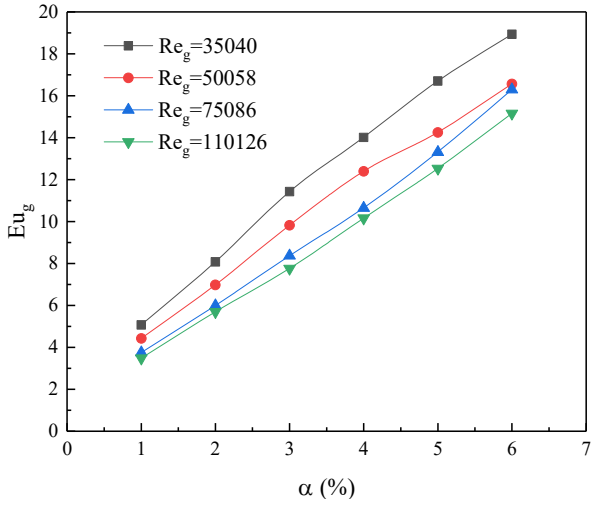

Fig. 14 Relationship between Eu_g and liquid volume fraction α

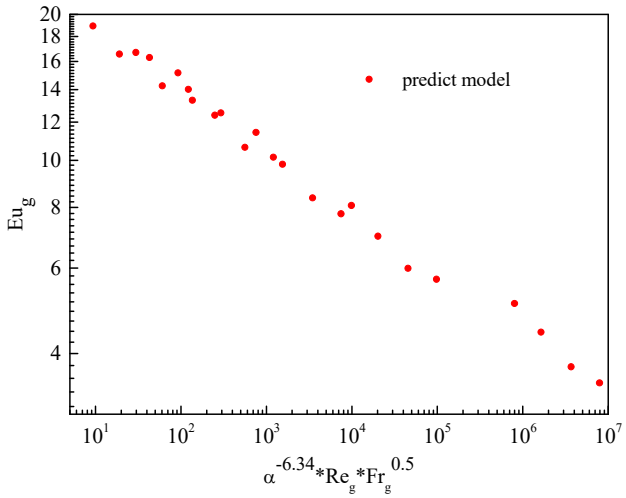

Fig. 15 Relationship between Eu_g and $a^{-6.34}$*Re_g*$Fr_g^{0.5}$

According to the above model, Fig. 16 shows the comparison of the model value and experimental data obtained by air-water in GLCC which almost all data fall within 10% of error bar.

2) The Natural Gas-Oil Two-Phase Flow in GLCC

The operating range was extended to industrial field where the fluids are natural gas and oil. The gas Euler number Eu_g at different inlet natural gas velocities and liquid volume fractions is shown in Figs. 17 and 18.

Fig. 17 shows the trend of the Euler number of the gas phase with the Reynolds number Re_g when the volume fraction is 1%, 2%,3%,4%,5%,6%. As can be seen from the figure, the Euler number of the gas phase Eu_g gradually decreases with the increase of the Reynolds number of the gas phase. And all of the cases finally tend to be same slope.

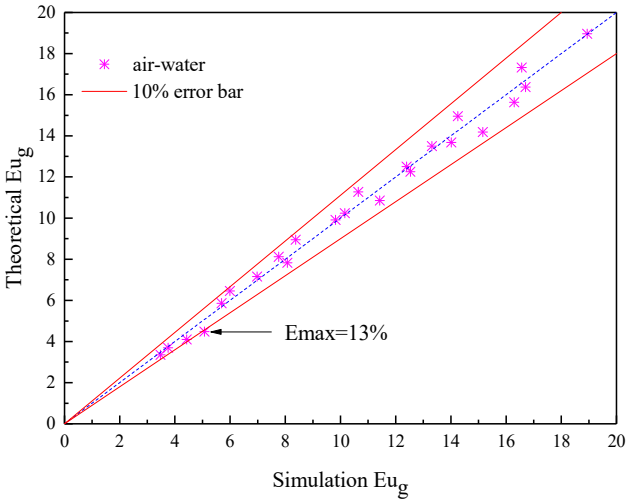

Fig. 16 Comparison of the model value and simulation data

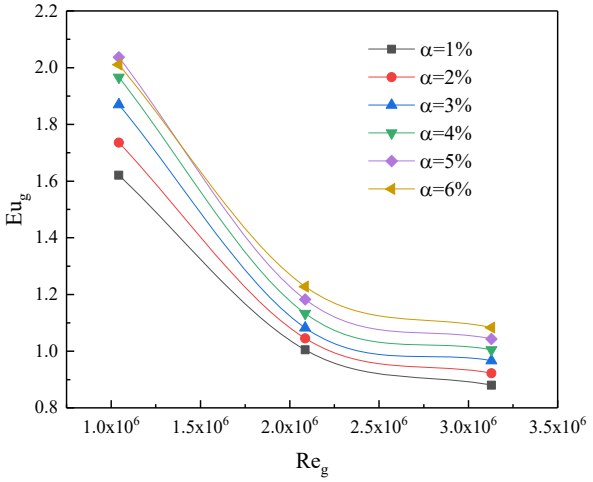

Fig. 17 Relationship between Eu_g and Re_g of GLCC

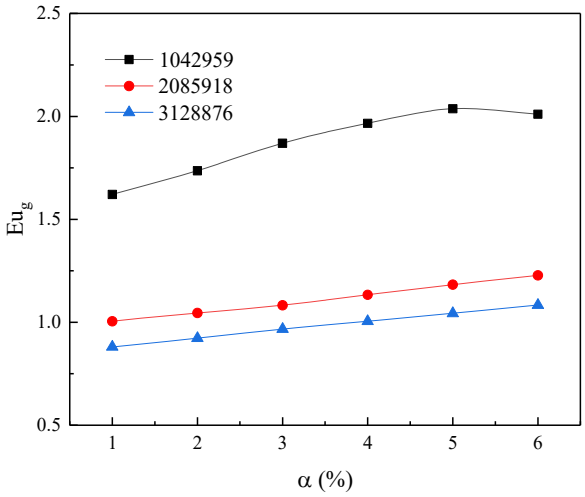

Fig. 18 Relationship between Eu_g and liquid volume fraction α

Fig. 18 shows the relationship between gas Euler number

Eu_g and liquid volume fraction when the Reynolds number of gas is 1042959, 2085918, and 3128876. It can be seen from the figure that the variation of Euler number Eu_g with liquid phase volume fraction approaches the linear relationship. And the slopes corresponding to each line are approximately equal.

Under natural gas-oil two-phase flow, the pressure drop prediction model can be assumed as following:

$$Eu_g = k_1 \alpha^{k2} \mathrm{Re}_g^{k3} Fr_g^{k4}$$

k_1, k_2, k_3 and k_4 are constant coefficients. Since the linear relationship exists between Eu_g and $a^{-0.4}*Re_g*Fr_g^{0.5}$ (Fig. 19), the mechanistic model is just like as following:

$$Eu_g = 246.7\alpha^{0.127} (\mathrm{Re}_g \sqrt{Fr_g})^{-0.320}, \quad 1.04\times10^6 < \mathrm{Re}_g < 3.13\times10^6$$

According to the above model, Fig. 20 shows the comparison of the model value and experimental data obtained by natural gas and oil in GLCC which almost all data fall within 10% of error bar.

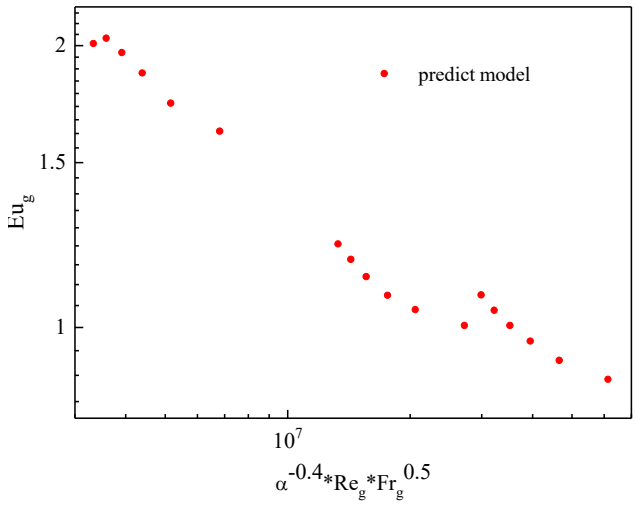

Fig. 19 Relationship between Eu_g and $a^{-0.4}*Re_g*Fr_g^{0.5}$

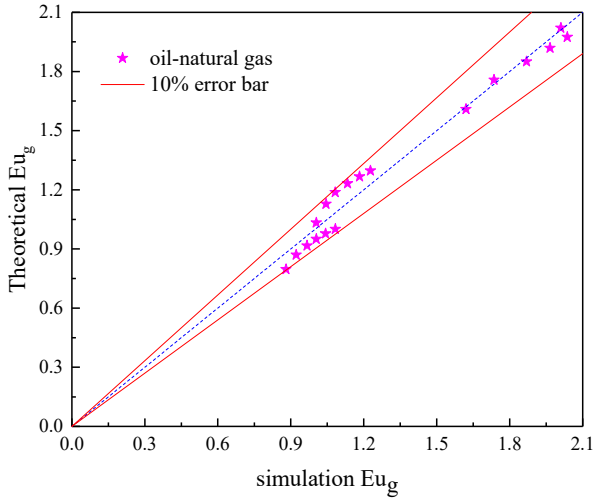

Fig. 20 Comparison of the model value and simulation data

V. Conclusions

The critical outputs of this study are summarized below:

1) For pure gas flow case, the Euler number of the gas phase Eu_g decreases with the increase of the Reynolds number of the gas phase. When Re is bigger than 1×10^6, the Eu number does not change with the increase of Reynolds number.
2) For gas liquid two phase flow, the Euler number of the gas phase Eu_g gradually decreases with the increase of the Reynolds number of the gas phase. And all the cases tend to follow the same slope at last.
3) The pressure drop is mainly focused on gas phase since the liquid fraction is too low to contribute much for it. Eu_g is a dimensionless number connected with gas phase pressure. The pressure drop model has been established as following:

$$Eu_g = f(Re_g, \alpha, Fr_g)$$

References

[1] J. Volckens and T. M. Peters, "Counting and particle transmission efficiency of the aerodynamic particle sizer," Journal of Aerosol Science, vol. 36, pp. 1400-1408, 2005.
[2] D. F. Bergman, M. R. Tek, and D. L. V. Katz, Retrograde condensation in natural gas pipelines: American Gas Association, 1975.
[3] R. Hreiz, R. Lainé, J. Wu, C. Lemaitre, C. Gentric, and D. Fünfschilling, "On the effect of the nozzle design on the performances of gas–liquid cylindrical cyclone separators," International Journal of Multiphase Flow, vol. 58, pp. 15-26, 2014.
[4] G. E. Kouba, O. Shoham, and S. Shirazi, "Design and performance of gas-liquid cylindrical cyclone separators," in Proceedings of the BHR Group 7th International Meeting on Multiphase Flow., Cannes, France, 1995, pp. 307-327.
[5] D. Farchi, "A study of Mixers and Separators for Two-phase flow in MHD Energy Conversion Systems," MS Thesis (in Hebrew), Ben-Gurion University, Israel, 1990.
[6] S. Movafaghian, J. Jaua-Marturet, R. S. Mohan, O. Shoham, and G. Kouba, "The effects of geometry, fluid properties and pressure on the hydrodynamics of gas–liquid cylindrical cyclone separators," International Journal of Multiphase Flow, vol. 26, pp. 999-1018, 2000.
[7] F. M. Erdal and S. A. Shirazi, "Effect of the inlet geometry on the flow in a cylindrical cyclone separator," Journal of Energy Resources Technology, vol. 128, pp. 62-69, 2006.
[8] F. M. Erdal, S. A. Shirazi, O. Shoham, and G. E. Kouba, "CFD simulation of single-phase and two-phase flow in gas-liquid cylindrical cyclone separators," SPE Journal, vol. 2, pp. 436-446, 1997.
[9] R. Hreiz, C. Gentric, and N. Midoux, "Numerical investigation of swirling flow in cylindrical cyclones," Chemical engineering research and design, vol. 89, pp. 2521-2539, 2011.
[10] A. J. Meléndez-Ramírez, M. A. Reyes-Gutiérrez, L. R. Rojas-Solórzano, J. C. Marín-Moreno, and J. Colmenares, "Experimental Study of a Gas-Liquid Cylindrical Cyclone Separator Performance," in ASME 2004 International Mechanical Engineering Congress and Exposition, 2004, pp. 755-761.
[11] F. Kaya and I. Karagoz, "Performance analysis of numerical schemes in highly swirling turbulent flows in cyclones," Current science, pp. 1273-1278, 2008.